BJ www.biochemj.org

BJ Structure

Biochem. J. (2012) **443**, 369–378 (Printed in Great Britain) doi:10.1042/BJ20112061

online data

A novel lectin from *Agrocybe aegerita* shows high binding selectivity for terminal *N*-acetylglucosamine

Shuai JIANG*, Yijie CHEN*, Man WANG*, Yalin YIN*, Yongfu PAN*, Bianli GU*, Guojun YU*, Yamu LI*, Barry Hon Cheung WONG*, Yi LIANG† and Hui SUN*‡§[1]

*College of Life Sciences, Wuhan University, Wuhan 430072, People's Republic of China, †Department of Clinical Immunology, Guangdong Medical College, Dongguan 523808, People's Republic of China, ‡Key Laboratory of Combinatorial Biosynthesis and Drug Discovery (Wuhan University), Ministry of Education, Wuhan 430071, People's Republic of China, and §State Key Laboratory of Virology, Wuhan University, Wuhan 430072, People's Republic of China

A novel lectin was isolated from the mushroom *Agrocybe aegerita* (designated AAL-2) by affinity chromatography with GlcNAc (*N*-acetylglucosamine)-coupled Sepharose 6B after ammonium sulfate precipitation. The AAL-2 coding sequence (1224 bp) was identified by performing a homologous search of the five tryptic peptides identified by MS against the translated transcriptome of *A. aegerita*. The molecular mass of AAL-2 was calculated to be 43.175 kDa from MS, which was consistent with the data calculated from the amino acid sequence. To analyse the carbohydrate-binding properties of AAL-2, a glycan array composed of 465 glycan candidates was employed, and the result showed that AAL-2 bound with high selectivity to terminal non-reducing GlcNAc residues, and further analysis revealed that AAL-2 bound to terminal non-reducing GlcNAc residues with higher affinity than previously well-known GlcNAc-binding lectins such as WGA (wheatgerm agglutinin) and GSL-II (*Griffonia simplicifolia* lectin-II). ITC (isothermal titration calorimetry) showed further that GlcNAc bound to AAL-2 in a sequential manner with moderate affinity. In the present study, we also evaluated the anti-tumour activity of AAL-2. The results showed that AAL-2 could bind to the surface of hepatoma cells, leading to induced cell apoptosis *in vitro*. Furthermore, AAL-2 exerted an anti-hepatoma effect via inhibition of tumour growth and prolongation of survival time of tumour-bearing mice *in vivo*.

Key words: *Agrocybe aegerita*, anti-hepatoma activity, fungal lectin, glycan-binding property, *N*-acetylglucosamine.

INTRODUCTION

Changes in glycosylation patterns play important roles in embryonic development, metabolic homoeostasis, pathogenic infections, immune surveillance and various diseases, including oncogenesis, diabetes and autoimmune disorders [1]. Therefore glycan analysis is of great importance for understanding the significance of glycan modifications. Lectins, with their diverse carbohydrate-binding properties, are potent tools for the study of glycan conjugates in various biological materials without glycan liberation. For example, lectins have been applied in the separation of cells at different stages, mitogenic activation of immune cells and identification of blood groups, as well as characterization of glycan alterations on the surface between normal and neoplastic cells [2–4].

The newly developed lectin array has been proved to be a powerful tool for the comprehensive analysis of glycans or glycoconjugates [5]. Much significant information has been obtained from use of lectin arrays. α1-2-Fucose-specific lectin (rBC2LCN) has been applied in the detection of undifferentiated induced pluripotent stem cells/embryonic stem cells, but not differentiated somatic cells [6], TKA (*Trichosanthes kirilowii* agglutinin) and PNA (peanut agglutinin) were used to distinguish the stem-like glioblastoma neurosphere cultured from a traditional adherent glioblastoma cell line [7], GNA (*Galanthus nivalis* agglutinin), NPA (*Narcissus pseudonarcissus* agglutinin), PSA (*Pisum sativum* agglutinin), LcH (*Lens culinaris* lectin) and Con A (concanavalin A) have been used for the detection of high-mannose N-linked oligosaccharides on differentiated neutrophils in comparison with the promyelocytic leukaemia cell line HL-60 [8], DSL (*Datura stramonium* lectin), SLL [*Solanum lycopersicum* lectin; formerly LEL (*Lycopersicon esculentum* lectin)] and MAL (*Maackia amurensis* lectin) showed a binding preference for mouse laminin, whereas SNA (*Sambucus nigra* agglutinin), SSA (*Salvia sclarea* agglutinin) and TJA-I (*Trichosanthes japonica* agglutinin-I) showed strong binding to bovine transferrin [9]. More lectins with unambiguous and/or distinctive glycan-binding selectivity are needed to be studied and exploited for probes of glycan structures. Thus there is an urgent need to find powerful lectin candidates for glycan analysis.

Lectins are useful tools for tumour diagnosis, antivirus research and drug-delivery studies [10]. For example, MAL has been used in prostate cancer diagnosis because of its preferential binding to prostate-specific antigen [11], HPA (*Helix pomatia* agglutinin) recognizes the glycosylation changes of metastatic breast cancer [12], BCA (*Boodlea coacta* lectin) can potently provide entry inhibition of HIV-1 and influenza viruses [13], microvirin has anti-HIV-1 activity with a high safety profile and low toxicity [14], and odorranalectin has been reported to be the smallest lectin so far and with potential for drug delivery and targeting

Abbreviations used: AAL-2, *Agrocybe aegerita* lectin 2; BLL, *Boletopsis leucomelas* lectin; GlcNAc, *N*-acetylglucosamine; GSL-II, *Griffonia simplicifolia* lectin-II; HPA, *Helix pomatia* agglutinin; IPTG, isopropyl β-D-thiogalactopyranoside; ITC, isothermal titration calorimetry; LacNAc, *N*-acetyl-lactosamine; MAL, *Maackia amurensis* lectin; MALDI, matrix-assisted laser-desorption ionization; MS/MS, tandem MS; nAAL-2, native AAL-2; ORF, open reading frame; PI, propidium iodide; PVL, *Psathyrella velutina* lectin; rAAL-2, recombinant AAL-2; RFU, relative fluorescence units; SLL, *Solanum lycopersicum* lectin; TBS, Tris-buffered saline; TOF, time-of-flight; WGA, wheatgerm agglutinin.

The nucleotide sequence data for *Agrocybe aegerita* lectin 2 will appear in the GenBank®, EMBL, DDBJ and GSDB Nucleotide Sequence Databases under accession number JN001164.

The glycan array data of AAL-2 were deposited in the Consortium for Functional Glycomics database with the labels primscreen_3312–primscreen_3315.

[1] To whom correspondence should be addressed (email sunhui@whu.edu.cn).

[15]. An increasing number of lectins from plants and animals have been purified and characterized; however, the information on lectins isolated from fungal sources remains limited [16]. Fungal lectins are attractive because of their wide distribution, high content, varied carbohydrate-binding specificities and especially anti-tumour activities. *Agaricus bisporus* lectin was shown to possess anti-tumour activity against human colon cancer HT29 and breast cancer cell lines MCF-7 [17], *Russula lepida* lectin exhibited anti-proliferative activity in hepatoma HepG2 cells and human breast cancer MCF-7 cells [18], *Tricholoma mongolicum* lectin-1 and lectin-2 could inhibit the growth of sarcoma 180 cells [19], *Pleurotus citrinopileatus* lectin exerted potent anti-tumour activity in mice bearing sarcoma 180 [20], and *Grifola frondosa* lectin was shown to be cytotoxic to HeLa cells [21].

In the present paper, we report a novel fungal lectin AAL-2 (*Agrocybe aegerita* lectin 2) from the fruiting body of *A. aegerita*. A glycan array analysis showed that AAL-2 bound to non-reducing GlcNAc (*N*-acetylglucosamine) termini with high selectivity, even higher than the previously well-known GlcNAc-binding lectins WGA (wheatgerm agglutinin) and GSL-II (*Griffonia simplicifolia* lectin-II), which have been widely used in biochemical and biomedical research. Moreover, we showed that AAL-2 had anti-tumour activity not only for the induction of hepatoma cells apoptosis *in vitro*, but also for the inhibition of H22 hepatoma growth and prolongation of survival times of tumour-bearing mice *in vivo*. The cloning and prokaryotic/bacterial protein expression of AAL-2 provided clues to the deep investigation of the glycan-binding mechanism of AAL-2 and further application of AAL-2 in probing GlcNAc-related glycans or glycoconjugates.

EXPERIMENTAL

Chemicals and reagents

The edible mushroom *A. aegerita* was collected from the Sanming Institute of Fungi (Sanming, Fujian, P.R. China). GlcNAc was purchased from Sangon Biotech. Epoxy-activated Sepharose 6B was purchased from GE Healthcare.

Cell lines and mice

A murine hepatoma cell line H22, and a human hepatoma cell line Huh7, were provided by the CCTCC (China Center for Type Culture Collection, Wuhan University). Male BALB/c mice (6–8-week-old) were purchased from the Hubei Experimental Animal Laboratory (Hubei, China) and maintained in a pathogen-free facility. Procedures were performed according to approved protocols and in accordance with recommendations for the proper care and use of laboratory animals.

Preparation of GlcNAc-coupled Sepharose 6B matrix

GlcNAc-coupled Sepharose 6B was prepared according to the manufacturer's instructions (GE Healthcare). In brief, 2 g of epoxy-activated Sepharose 6B was washed twice with 200 ml of distilled water, mixed with GlcNAc at a final concentration of 200 μmol/ml in distilled water (pH 13) at a temperature of 30 °C for 15 h. Free remaining groups were blocked by incubating in 1 M ethanolamine, and the mixture was gently agitated at 45 °C for 4 h. The Sepharose 6B-coupled GlcNAc matrix was washed extensively with TBS (Tris-buffered saline) (pH 7.2) and packed into an empty 100-mm-long glass column with a 10 mm inner diameter. The column was stored at 4 °C until use.

Purification of AAL-2 from mushroom *A. aegerita*

Dried *A. aegerita* fruiting bodies were crushed into a powder, and 50 g of the dried mass was dissolved and extracted three times with 1 litre of distilled water at 4 °C. The extracts were pooled and centrifuged at 10000 ***g*** for 15 min. Solid ammonium sulfate was added to the supernatant to 40 % saturation and centrifuged again at 10000 ***g*** for 15 min. Solid ammonium sulfate was then added to the supernatant to obtain 80 % saturation, and the 40–80 % precipitate was collected by centrifugation at 10000 ***g*** for 15 min. The precipitated protein was dissolved in 200 ml of distilled water and dialysed extensively against 50 mM TBS (pH 7.2) by changing the dialysis buffer three times at 4 °C overnight. The sample was loaded on to an affinity column (GlcNAc-coupled Sepharose 6B matrix) pre-equilibrated with TBS (pH 7.2), and eluted with 0.2 M GlcNAc in 50 mM TBS (pH 7.2) after extensive washing with TBS. The enriched AAL-2 fraction was stored at − 20 °C.

SDS/PAGE was performed with a 15 % acrylamide running gel and 5 % stacking gel. Protein bands were identified by Coomassie Brilliant Blue R-250 staining.

Preparation of tryptic peptides and peptide sequencing

The band corresponding to AAL-2 was excised from a Coomassie Brilliant Blue-stained SDS/polyacrylamide gel and tryptically digested according to standard protocols. The peptides were derivatized for the N-terminus with SPITC (4-sulfophenyl isothiocyanate) and desalted with ZipTip™. MALDI (matrix-assisted laser-desorption ionization)–MS was performed on a 4700-Proteomics Analyzer (Applied Biosystems) and PSD (power spectral density) spectra were collected with 3000 laser shots at 1 keV collision energy without CID (collision-induced dissociation). MS data were analysed by PMF (peptide mass fingerprinting) using MASCOT software.

Molecular mass determination by MS

MALDI–TOF (time-of-flight) mass spectra were obtained using a Voyager-RP mass spectrometer (PerSeptive Biosystems) [22].

cDNA cloning of *AAL-2* and expression of rAAL-2 (recombinant AAL-2) in *Escherichia coli*

Total RNA was prepared from the fresh fruiting bodies of *A. aegerita* by grinding in liquid nitrogen followed by extraction with Plant RNA Isolation Reagent (BioTeke). Full-length cDNAs were synthesized from 1 μg of total RNA using MMLV (Moloney murine leukaemia virus) reverse transcriptase (Promega) after RQ1 RNase-free DNase digestion (Promega) according to the manufacturer's instructions. Nested PCR was applied to amplify the AAL-2 coding sequence, and two pairs of primers were designed as follows: forward external primer *aal-2*_5′_F1, 5′-ATGAACGTGAACGTGGGAGG-3′; reverse external primer *aal-2*_3′_R1, 5′-CTAGTAATCCGTGCGAGTCG-3′; forward ORF (open reading frame) primer *aal-2*_5′_F2, 5′-ATGACCAGCAACGTCATCAC-3′; reverse ORF primer *aal-2*_3′_R2, 5′-ATGCCTGCTGCTGTCCAAGT-3′. PCR was performed using Taq DNA polymerase (Promega) with the following temperature profile: 5 min at 95 °C, 30 s at 94 °C and 3 min at 72 °C, for 35 cycles. The amplified product obtained with external primers was used as the template for a second round of amplification with the ORF primers. The purified PCR fragment was cloned into the pET-30a vector (Novagen) according to the manufacturer's instructions. The resulting plasmid containing rAAL-2 coding sequence was used

for transformation into *E. coli* BL21 cells (Novagen). Induction of protein expression was performed with 1 mM IPTG (isopropyl β-D-thiogalactopyranoside) at mid-exponential phase (D_{600} of 0.4–0.6), and the bacteria were grown for an additional 5 h at 37 °C with shaking at 220 rev./min. The bacteria were then harvested and lysed. The supernatant was loaded on to a GlcNAc–Sepharose 6B column, and rAAL-2 was purified by GlcNAc-coupled Sepharose 6B affinity chromatography as described above.

Biotinylation of AAL-2

To biotinylate AAL-2, purified AAL-2 (200 μg in 250 μl of PBS) was mixed with 400 μl of biotin ester solution (100 μg of biotin ester/200 μg of lectin) and left for 30 min at room temperature (24 °C). The biotin-labelled AAL-2 was collected using Sephadex G-250 and stored at − 20 °C until use.

Glycan array analysis

To determine the carbohydrate-binding specificity of AAL-2, glycan array analysis was performed by the Consortium for Functional Glycomics (Core H; http://www.functionalglycomics.org/static/consortium/resources/resourcecoreh.shtml). The printed glycan array (Mammalian Printed Array version 4.1) [23] was composed of 465 different natural and synthetic mammalian glycans. In the binding assay, array slides, containing six replicates per glycan or glycoconjugate, were incubated with different concentrations of biotinylated AAL-2 (0.1, 1, 50 and 200 μg/ml). The slides were then washed, and bound lectin was detected using fluorescently labelled streptavidin. Array slides were subjected to imaging, and the fluorescence was measured as described previously [24]. Briefly, fluorescence intensity was detected using a ScanArray 5000 confocal scanner (PerkinElmer). ImaGene® image analysis software (BioDiscovery) was used to analyse the image. The relative binding for each glycan was expressed as mean RFU (relative fluorescence units) of four of the six replicates.

ITC (isothermal titration calorimetry)

ITC experiments on the interaction of GlcNAc with AAL-2 were performed at 25 °C with a VP-ITC isothermal titration calorimeter (Microcal). Freshly purified AAL-2 was dialysed overnight in PBS (pH 7.2) at 4 °C. The protein concentration in the microcalorimeter cell (1.4478 ml volume) was 50 μM. GlcNAc solution was made up to 7 mM in PBS and placed in the syringe. The first injection (4 μl) was followed by 27 injections of 10 μl, and the stirring rate was set at 300 rev./min. The dilution heat of the GlcNAc was measured by injecting GlcNAc solution into buffer alone and was subtracted from the experimental curves before data analysis. The experimental data were fitted to a theoretical titration curve using Microcal Origin software supplied with the instrument, and the standard molar enthalpy change for the binding, $\Delta_b H_m^0$, and the dissociation constant, K_d, were derived. The standard molar free energy change, $\Delta_b G_m^0$, and the standard molar entropy change, $\Delta_b S_m^0$, for the binding reaction were calculated by using the following thermodynamic equations:

$$\Delta_b G_m^0 = RT \cdot \ln K_d \quad (1)$$

$$\Delta_b S_m^0 = \left(\Delta_b H_m^0 - \Delta_b G_m^0\right)/T \quad (2)$$

Haemagglutination assay

The haemagglutination activity of purified lectin was determined as described previously [25]. Briefly, the haemagglutination activity assay was performed on a microtitre plate, and the lectin sample (50 μl, 1 mg/ml) was serially diluted with PBS and mixed with 50 μl of a 2 % suspension of chicken red blood cells at room temperature. Measurements were taken after 30 min when the control (no lectin added) was fully precipitated.

The effects of metal cations on the haemagglutination activity of AAL-2 were determined in the absence and presence of 10 mM Ca^{2+}, Zn^{2+}, Mn^{2+} or Mg^{2+} after dialysis against 20 mM EDTA. The effect of temperature on lectin stability was monitored over a temperature range by incubation with AAL-2 for 30 min at each temperature. The samples were then cooled rapidly and assayed for haemagglutination activity. The effect of pH on lectin stability was determined by incubating with AAL-2 with buffers of different pHs for 30 min, and haemagglutination activity was determined after neutralization.

Preparation of a polyclonal anti-AAL-2 antibody

A rabbit polyclonal antibody against AAL-2 was prepared as reported previously [26]. Briefly, 500 μg of nAAL-2 (native AAL-2) in 500 μl of PBS was emulsified with 500 μl of complete Freund's adjuvant (Sigma). The emulsion was injected into 6-month-old New Zealand White rabbits by multipoint subcutaneous implantation. The second and third inoculations were performed on days 24 and 36 with Freund's incomplete adjuvant (Sigma), and the fourth inoculation was performed on day 41 without any adjuvant. At 1 week after the final immunization, sera were separated from the collected blood samples and antibody against nAAL-2 was detected by ELISA.

Cell culture

H22 cells and Huh7 cells were cultured in RPMI 1640 medium and DMEM (Dulbecco's modified Eagle's medium) respectively. Cell culture media were supplemented with 10 % (v/v) heat-inactivated (56 °C, 30 min) FBS (fetal bovine serum), 5 units/ml penicillin and 50 μg/ml streptomycin. All cells were maintained at 37 °C in a humidified atmosphere containing 5 % CO_2. For all experiments, cells were plated 2 h before treatment to allow for adherence.

Cell-adhesion assay, Annexin V/PI (propidium iodide) staining and FACS analysis

In the cell-adhesion assay, H22 and Huh7 cells were incubated with or without AAL-2, and then with polyclonal antibody against AAL-2 and FITC-conjugated goat anti-rabbit IgG. For Annexin V/PI staining, H22 and Huh7 cells were treated with AAL-2 at final concentrations of 0, 0.6, 1.2 or 2.4 μM for 24 and 36 h respectively. The cells were collected, washed twice with ice-cold PBS (pH 7.4), and stained using an Annexin V/PI apoptosis kit (MultiScience Biotech). The samples were mixed gently and incubated in the dark. All samples were analysed by flow cytometry (Beckman, Epics Altra)

Subcutaneous tumour models

H22 cells (10^7) in 100 μl of PBS were subcutaneously injected into the right flank of BALB/c mice. At days 7, 9, 11, 13, 15, 17 and 19 after tumour inoculation, mice were injected at the tumour site with 5 mg of AAL-2/kg in 100 μl of PBS or diluent control.

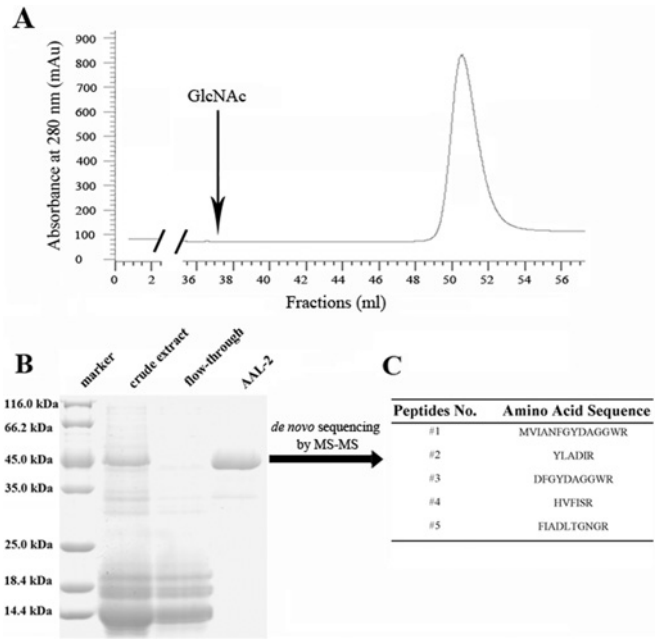

Figure 1 Purification of AAL-2 and the amino acid sequences of tryptic peptides identified by MS

(**A**) Crude extract was applied to a GlcNAc monomer-coupled epoxy-activated Sepharose 6B column (1 cm × 10 cm) and equilibrated with TBS (pH 7.2). After washing with TBS, AAL-2 was eluted with TBS containing 0.2 M GlcNAc (indicated by the arrow). The plot was generated by ÄKTAprime (GE Healthcare). (**B**) SDS/polyacrylamide gel of AAL-2 was stained with Coomassie Brilliant Blue. Molecular masses are indicated in kDa. (**C**) Amino acid sequence data for AAL-2. The five tryptic peptides identified by MS/MS are shown.

Tumour volume (V) was determined by caliper measurements ($V = L \times W^2/2$), where L is length and W is width.

Statistical analysis

The two-sample Student's *t* test was used for comparisons between groups. Statistical analysis was performed with GraphPad Prism 5 software. Results are means ± S.E.M., and statistical significance was defined as $P < 0.05$.

RESULTS

Purification of AAL-2 and the determination of the amino acid sequences from AAL-2 tryptic peptides

Total crude proteins were extracted from dried *A. aegerita* fruiting bodies by water-extraction, 40–80 % ammonium sulfate precipitation and dialysis against TBS. The total crude proteins were loaded on to the GlcNAc-coupled Sepharose 6B column and eluted with 0.2 M GlcNAc after extensive TBS washing (Figure 1A). A total fraction of 6 ml of eluate (48–54 ml) was collected. Representative purification fractions from the affinity chromatographic column were separated by SDS/PAGE in the presence of 2-mercaptoethanol. The eluate fraction yielded a single band (approximately 43 kDa) and was named AAL-2 (Figure 1B). AAL-2 was characterized further using *de novo* sequencing by MS/MS (tandem MS), and five tryptic peptides were identified (Figure 1C). The five peptide sequences were analysed further by BLASTP at NCBI (http://www.ncbi.nlm.nih.gov/BLAST), and only two peptides (labelled #1 and #3) showed homology with the GlcNAc-binding lectin PVL (*Psathyrella velutina* lectin) [27] (results not shown).

Identification of the AAL-2 coding sequence

To determine the coding sequence of AAL-2, the *A. aegerita* transcriptome was sequenced. Raw Illumina sequencing data of the *A. aegerita* transcriptome was deposited in the Sequence

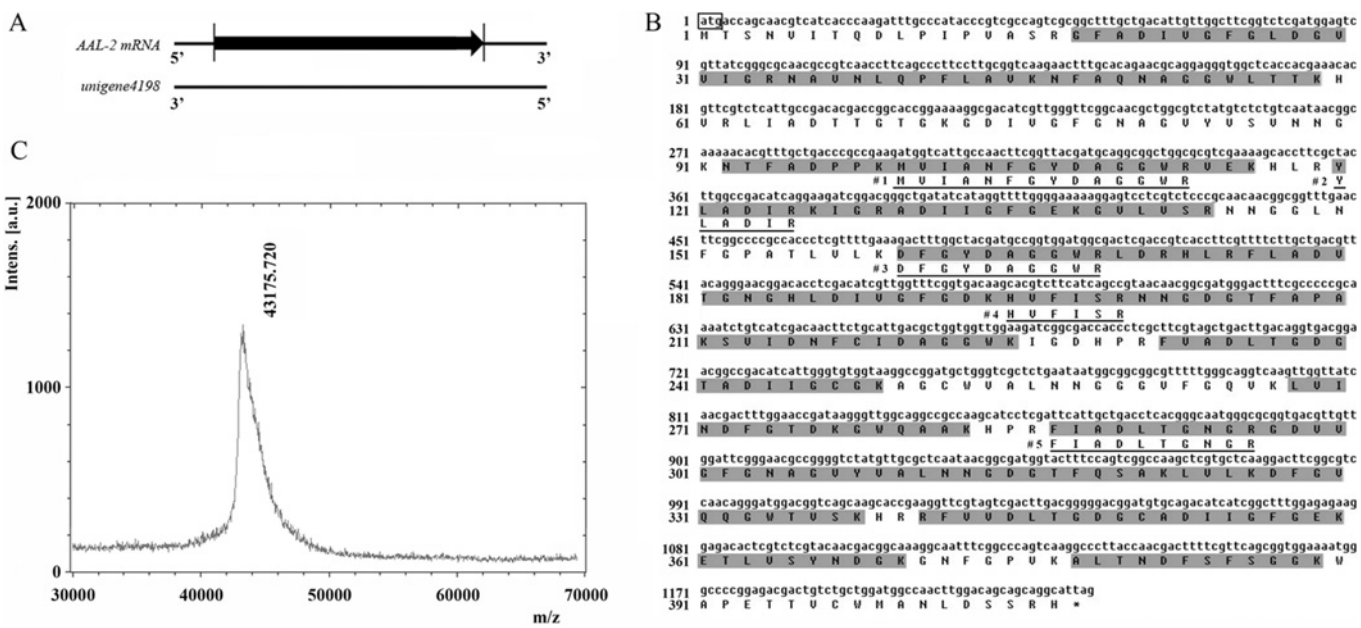

Figure 2 Identification of AAL-2 coding sequence

(**A**) The AAL-2 coding sequence is located on the complementary strand of UniGene 4198. (**B**) The AAL-2 coding sequence consists of 1224 bp, which is computationally translated into 407 amino acids. The deduced amino acid sequence is shown under the AAL-2 coding sequence, and the five tryptic peptides (underlined) of AAL-2 identified by MS are aligned under the deduced amino acid sequence. MALDI–TOF/TOF analysis revealed 69 % sequence coverage of the full-length AAL-2 (grey box). The initiation codon ATG is boxed and the stop codon tag is marked with an asterisk. (**C**) Determination of AAL-2 molecular mass by MALDI–TOF-MS to be 43175.72 Da. Intens., intensity (in arbitrary units, a.u.).

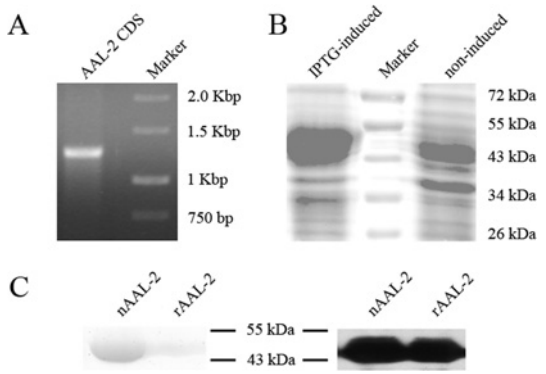

Figure 3 Cloning, expression and purification of AAL-2

(**A**) Total RNA was isolated from fresh *A. aegerita* fruiting body and amplified by reverse transcription–PCR. The AAL-2 coding sequence (~1.2 kb) was amplified by nested PCR. (**B**) The AAL-2 coding sequence was cloned into pET-30a plasmids followed by transformation into *E. coli* BL21 cells. A strong band appeared at approximately 43 kDa after IPTG-induction for 5 h compared with non-induction. (**C**) nAAL-2 and rAAL-2 showed the same electrophoretic mobility on SDS/PAGE and shared the same immunogenicity after immunoblotting with the anti-nAAL-2 polyclonal antibody. Molecular masses are indicated in kDa.

Read Archive at NCBI (accession number SRA026731.1). The five tryptic AAL-2 peptides were searched for similarity against the *A. aegerita* transcriptome by BLASTX. The ORF of the complementary strand of UniGene 4198 was analysed, and a fragment containing 1224 bp was identified and labelled as the AAL-2 coding sequence (Figures 2A and 2B). Five tryptic peptides (underlined) from AAL-2 showed full homology with the protein translated from the identified AAL-2 coding sequence, with the latter MALDI–TOF/TOF analysis showing 69 % coverage (Figure 2B, grey box); moreover, the molecular mass was calculated to be 43175 Da by the ExPASy Proteomics Server (http://www.expasy.org/tools), and was consistent with the AAL-2 mass (43175.72 Da) identified by MALDI–TOF-MS (Figure 2C). The isoelectric point of AAL-2 was calculated to be 8.19 by ExPASy.

Cloning of AAL-2 coding sequence and rAAL-2 protein expression

The AAL-2 coding sequence was successfully cloned after nested PCR using total cDNA as a template (Figure 3A). The nucleotide sequence of the cloned AAL-2 coding sequence was fully identical with that from the *A. aegerita* transcriptome. The AAL-2 coding sequence was then cloned into the expression vector pET-30a, and the resulting plasmid was used for the transformation of *E. coli* BL21 cells. The bacteria were grown to mid-exponential phase (D_{600} of 0.4–0.6) and then induced with 1 mM IPTG. After 5 h of induction, the lysate of the bacteria was separated by SDS/PAGE, and a strong band of approximately 43 kDa appeared compared with non-induced bacteria (Figure 3B). The supernatant fractions from the lysate were loaded on to the GlcNAc-coupled Sepharose 6B column. rAAL-2 was eluted as a single symmetrical peak at the same elution volume as nAAL-2 (results not shown), and produced an electrophoretic mobility by SDS/PAGE identical with that of nAAL-2 at approximately 43 kDa. In addition, polyclonal antibody raised against nAAL-2 was able to detect rAAL-2, and a precipitin band was formed identical with that of nAAL-2 (Figure 3C).

Analysis of the carbohydrate-binding properties of AAL-2 characterized by glycan array and ITC

The purification of AAL-2 by affinity chromatography showed that AAL-2 was able to bind to GlcNAc. To characterize further

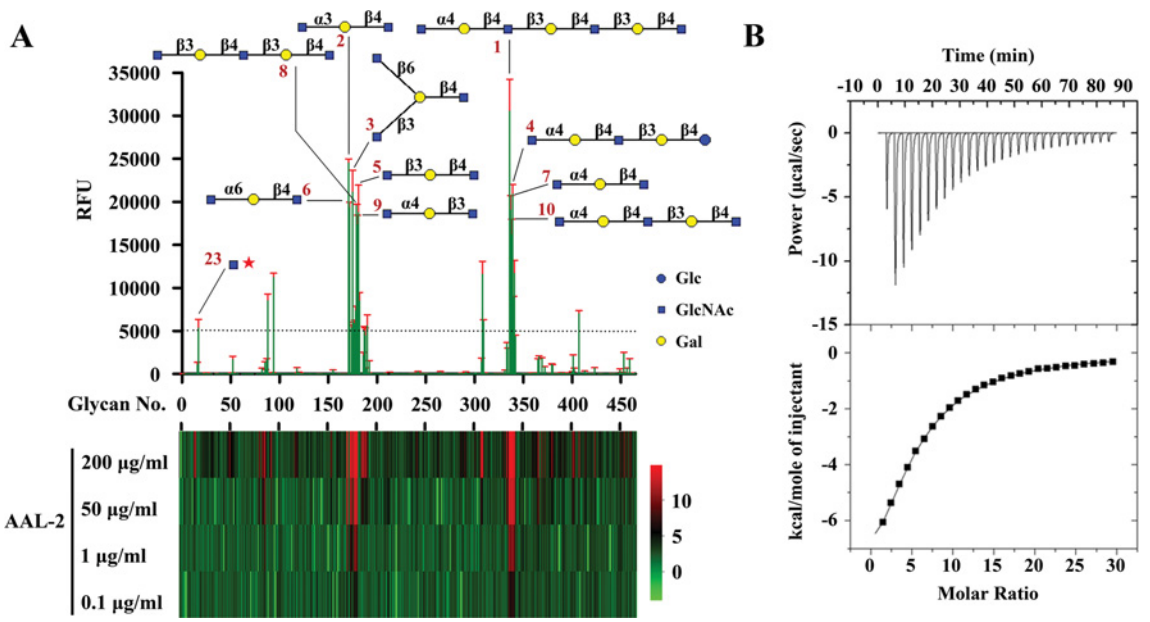

Figure 4 Binding properties of AAL-2 for GlcNAc assessed by glycan array analysis and ITC profiling

AAL-2-binding specificity was determined by glycan screening on a printed array (Version 4.1 of the Consortium for Functional Glycomics). (**A**) Upper panel: the top ten glycans with highest binding affinity to AAL-2 (200 μg/ml). The binding glycan GlcNAc is shown and labelled with a red asterisk. Results are means ± S.E.M. The glycan number at the bottom indicates the various glycans used in the glycan array. The entire glycan array is available at http://www.functionalglycomics.org/static/consortium/resources/resourcecoreh14.shtml. Lower panel: the heat map shows the binding selectivity of AAL-2 at different concentrations (0.5, 1, 50 and 200 μg/ml). The log (base 2) of RFU values is represented on the bar on the right-hand side. Warmer colours indicate higher binding affinity. (**B**) ITC results for GlcNAc monomer (7 mM) binding to AAL-2 (0.05 mM) in PBS at 25 °C. Upper panel: data obtained from 28 automatic injections of 10 μl of GlcNAc monomer each into the AAL-2-containing cell. Lower panel: plot of the total heat released as a function of ligand concentration for the titration shown above (squares). The continuous line represented the best least-squares fit to the obtained data. All thermodynamic measurements of AAL-2 binding to GlcNAc were performed at 25 °C.

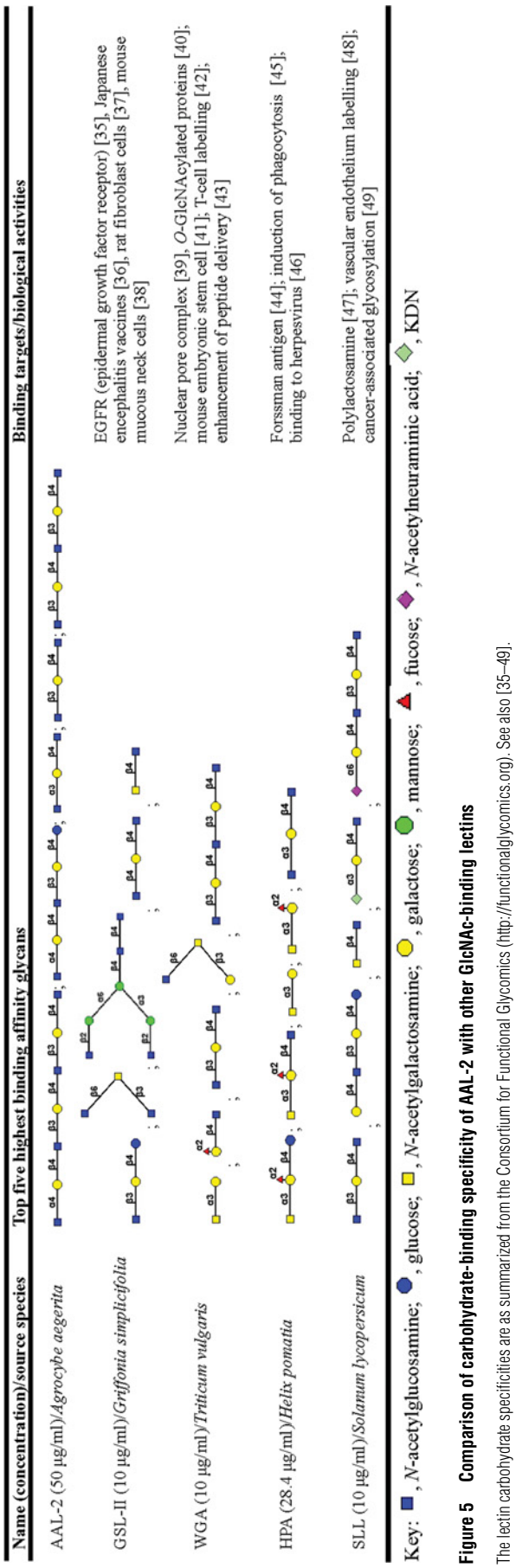

Figure 5 Comparison of carbohydrate-binding specificity of AAL-2 with other GlcNAc-binding lectins

The lectin carbohydrate specificities are as summarized from the Consortium for Functional Glycomics (http://functionalglycomics.org). See also [35–49].

the glycan-binding profile of AAL-2, glycan array analysis was performed by testing the binding affinity of AAL-2 to 465 glycan candidates. The glycan array was performed at different concentrations (0.1, 1, 50 and 200 μg/ml) of AAL-2, and the binding glycans with more than 5000 RFU were listed according to the glycan-binding profile of AAL-2 at 200 μg/ml (Supplementary Table S1 at http://www.BiochemJ.org/bj/443/bj4430369add.htm). The results showed that the binding selectivity changed little with a wide concentration range (Figure 4A, lower panel). Almost all of the top 30 glycans in the binding profiles possessed terminal non-reducing GlcNAc (Figure 4A, upper panel, and Supplementary Figure S1 at http://www.BiochemJ.org/bj/443/bj4430369add.htm). In addition, Gal (galactose)–GlcNAc [LacNAc (*N*-acetyl-lactosamine)] linked behind would increase the binding affinity to the terminal GlcNAc, and the glycan GlcNAc-$(LacNAc)_3$ exhibited the highest binding affinity among the 465 glycan candidates (Figure 4A, upper panel). However, $(LacNAc)_3$, with the absence of the terminal GlcNAc compared with GlcNAc-$(LacNAc)_3$, showed significantly low binding affinity. In comparison with other GlcNAc-binding lectins (Figure 5), AAL-2 performed better than the well-known GlcNAc-binding lectins WGA and GSL-II, which have been used widely in glycan studies for their high GlcNAc-binding selectivity. Therefore AAL-2 can be defined as a lectin with high binding selectivity to glycans with non-reducing GlcNAc termini and has potential in GlcNAc-related glycan or glycoconjugate analysis.

ITC was also performed in order to thermodynamically characterize the GlcNAc and AAL-2 interactions. Figure 4(B) (upper panel) shows the raw ITC curve resulting from the injection of GlcNAc into a solution of AAL-2. The titration curve showed that GlcNAc binding to AAL-2 was exothermic, resulting in negative peaks in the plots of power against time. Figure 4(B) (lower panel) shows the plot of the heat evolved per mol of GlcNAc added, with the heat of GlcNAc dilution subtracted. Our calorimetric data were fitted to a sequential binding model, and the thermodynamic parameters for the binding of GlcNAc to AAL-2 are summarized in Table 1. The values of K_{d1} and K_{d2} are 195 and 459 μM respectively, which indicates that GlcNAc bound to AAL-2 with moderate binding affinity.

AAL-2 can induce apoptosis in hepatoma cells *in vitro*

AAL-2 could bind to H22 and Huh7 hepatoma cells (Figures 6A and 6B) and induce apoptosis of H22 cells and Huh7 cells *in vitro*.

Table 1 Thermodynamic parameters for the binding of AAL-2 to GlcNAc as determined by ITC

Thermodynamic parameters, K_d and $\Delta_b H_m{}^0$, were determined by using the sequential binding sites model. The standard molar binding free energy ($\Delta_b G_m{}^0$) and the standard molar binding entropy ($\Delta_b S_m{}^0$) for the binding reaction were calculated using eqns (1) and (2) respectively. The buffer used in the assay was PBS (pH 7.2), ITC measurements was performed at 25 °C. Results are means ± S.E.M. 1 cal = 4.184 J.

Thermodynamic parameter (unit)	Value
K_{a1} (10^3 M^{-1})	5.13 ± 0.36
K_{a2} (10^3 M^{-1})	2.18 ± 0.06
K_{d1} (μM)	194.93 ± 70.16
K_{d2} (μM)	458.72 ± 27.52
$\Delta_b H_{m1}{}^0$ (kcal · mol^{-1})	− 32.22 ± 1.91
$\Delta_b H_{m2}{}^0$ (kcal · mol^{-1})	− 31.69 ± 2.24
$\Delta_b G_{m1}{}^0$ (kcal · mol^{-1})	− 5.06 ± 0.21
$\Delta_b G_{m2}{}^0$ (kcal · mol^{-1})	− 4.56 ± 0.04
$\Delta_b S_{m1}{}^0$ (cal · mol^{-1} · K^{-1})	− 91.08 ± 1.92
$\Delta_b S_{m2}{}^0$ (cal · mol^{-1} · K^{-1})	− 91.01 ± 2.24

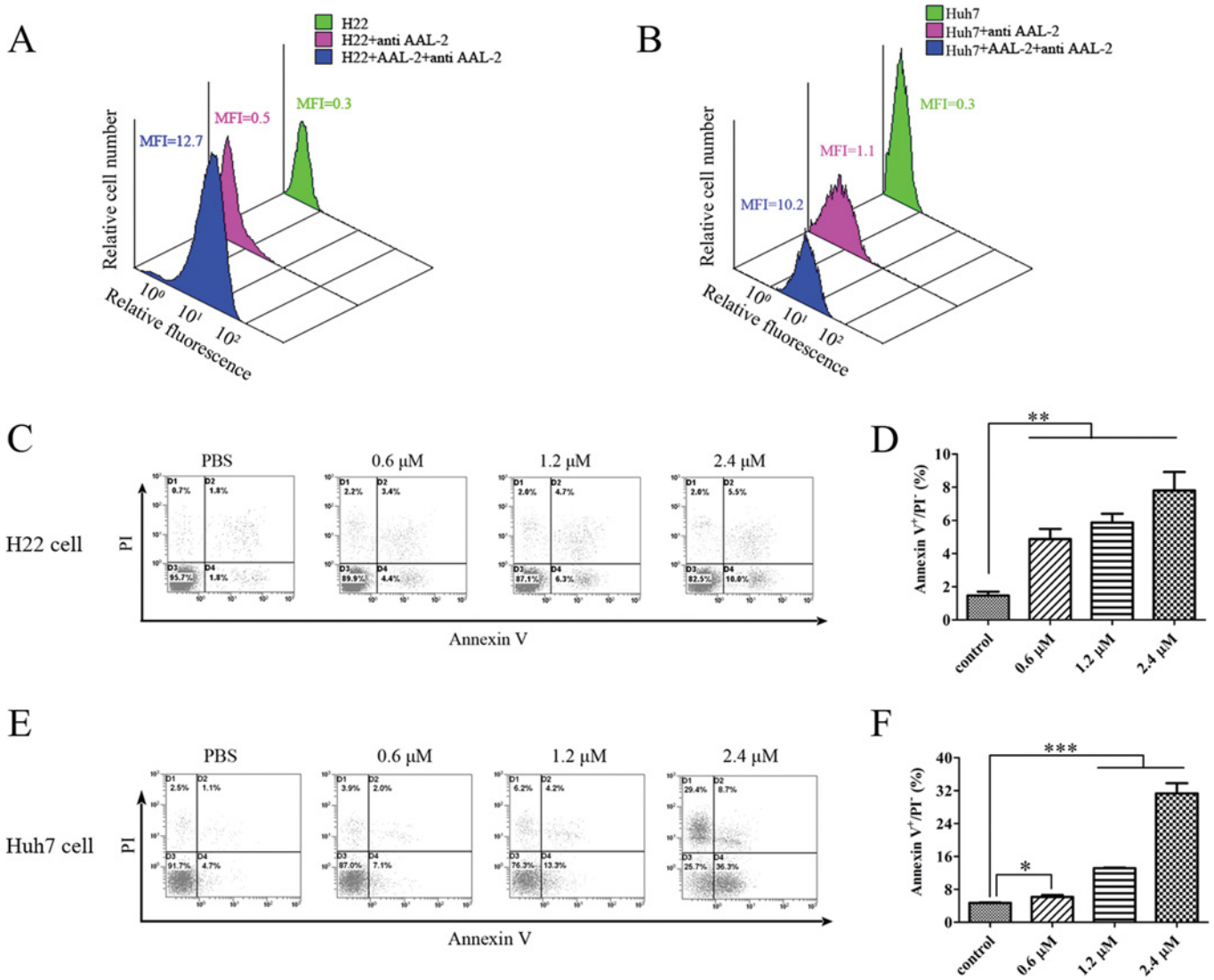

Figure 6 AAL-2 induces apoptosis in hepatoma cells *in vitro*

AAL-2 could bind to H22 (**A**) and Huh7 (**B**) hepatoma cells. H22 cells and Huh7 cells were untreated (green histograms), incubated with the anti-AAL-2 antibody alone (pink histograms), or with both AAL-2 and anti-AAL-2 antibody (blue histograms), and analysed by flow cytometry. The mean fluorescence intensity (MFI) values of the different incubation conditions are indicated in each histogram. Apoptotic H22 (**C**) and Huh7 (**E**) cells were detected by Annexin V/PI staining after 24 and 36 h of incubation respectively with different concentrations of AAL-2. The percentages of pro-apoptotic H22 cells (**D**) and Huh7 cells (**F**) gated on Annexin V^+/PI^- were calculated. Results are means ± S.E.M. ($n = 3$); $^*P < 0.05$, $^{**}P < 0.01$, $^{***}P < 0.001$.

The amount of apoptosis of H22 cells was 1.8 % after 24 h of culture, and increased significantly to 4.4 %, 6.3 % and 10 % at final concentrations of 0.6, 1.2 and 2.4 μM respectively (Figures 6C and 6D). Similarly, the proportion of apoptotic Huh7 cells was 4.7 %, and increased to 7.1 %, 13.3 % and 36.3 % when treated with AAL-2 at final concentrations of 0.6, 1.2 and 2.4 μM respectively for 36 h (Figures 6E and 6F). The results indicate that AAL-2 induced cell apoptosis in a concentration-dependent manner.

AAL-2 can inhibit hepatoma growth and extend the survival time of tumour-bearing mice *in vivo*

The anti-hepatoma activity of AAL-2 was investigated further by using a mouse model of H22 hepatocellular carcinoma. Mice treated with AAL-2 showed a significant reduction in tumour volume (Figure 7B), whereas body weight remained unaltered (Figure 7A) compared with control mice treated with PBS. In addition, AAL-2 treatment was able to extend the survival time of tumour-bearing mice (Figure 7C). Overall, we conclude that AAL-2 has anti-hepatoma activity by inhibiting hepatocellular carcinoma growth and can extend survival times of tumour-bearing mice.

DISCUSSION

A. aegerita is one of the most cultivated mushrooms in China, and has been highly valued as a functional food for its anti-tumour and nutritional benefits [28]. We have previously purified AAL (*A. aegerita* lectin) from *A. aegerita*, which showed extensive anti-tumour activity owing to specific binding to the Thomsen–Friedenreich disaccharide tumour antigen and subsequently resulted in tumour cell apoptosis [29,30]. In the present study, a novel fungal lectin AAL-2 was purified from *A. aegerita* by using one-step affinity chromatography. AAL-2 showed high binding

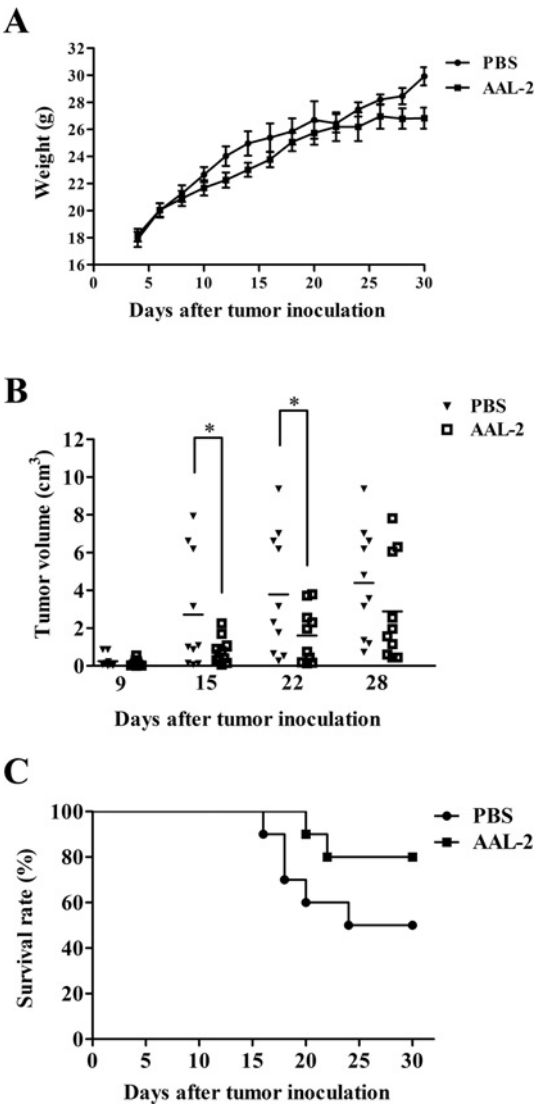

Figure 7 AAL-2 inhibits hepatocellular carcinoma growth and prolongs survival time of tumour-bearing mice *in vivo*

A total of 10^7 H22 cells were injected subcutaneously into the right flank of BALB/c mice. On days 7, 9, 11, 13, 15, 17 and 19 after tumour inoculation, mice were injected at the tumour site with 5 mg of AAL-2/kg in 100 μl of PBS or diluent control. Tumour-bearing mice treated with AAL-2 and PBS were monitored for changes in body weight (**A**), tumour growth (**B**) and survival time (**C**). Results are means $\pm$ S.D. ($n = 10$); $^*P < 0.05$.

selectivity to glycans with a non-reducing GlcNAc terminus, and the binding affinity increased when one or more LacNAc disaccharides were linked to the terminal GlcNAc via α1-3, α1-4 or β1-3, β1-4 linkages to form a GlcNAc-$(LacNAc)_{1-3}$ structure, implying that the addition of a LacNAc could increase the binding affinity to terminal GlcNAc (Supplementary Table S1). The glycan GlcNAc-$(LacNAc)_3$ represented the highest binding affinity among the 465 candidates; however, the high binding affinity would be lost if the terminal GlcNAc was removed. In addition, the binding selectivity changed little at a wide concentration range of AAL-2, indicating that the glycan-binding activity of AAL-2 was highly selective, low noise and was not affected by the high concentration (200 μg/ml) (Figure 4A, lower panel).

Our glycan array analysis revealed that AAL-2 bound to terminal GlcNAc with high selectivity. We then compared further the glycan-binding specificity of AAL-2 with that of other GlcNAc-binding lectins: PVL, BLL (*Boletopsis leucomelas* lectin), GSL-II, WGA, HPA and SLL. The GlcNAc-binding specificity of PVL was determined by affinity chromatography, and PVL was shown to have preferential binding to oligosaccharides bearing non-reducing terminal β-GlcNAc linked 1-6 or 1-3, but poor affinity for 1-4 linkages [27], whereas AAL-2 bound preferentially to oligosaccharides bearing a non-reducing terminal β-GlcNAc linked via a 1-4 or 1-3, rather than a 1-6, linkage. The unique structure of carbohydrate-binding domains might contribute to the binding preference of AAL-2 to terminal β-GlcNAc-linked oligosaccharides; our future studies will focus on the analysis of the carbohydrate–lectin interactions via crystallization of the AAL-2 and GlcNAc complex. The GlcNAc-binding specificity of BLL was determined by frontal affinity chromatography, and BLL was shown to have high binding affinity for mono-, bi- and tri-antennary agalactosylated glycans [31], whereas AAL-2 showed high binding affinity for mono-terminal non-reducing GlcNAc residues. Other GlcNAc-binding lectins, i.e. GSL-II, WGA, HPA and SLL, with their top five highest binding glycans from the glycan array data are listed in Figure 5. The comparative analysis showed that AAL-2 and GSL-II had the highest binding selectivity for terminal GlcNAc, whereas AAL-2 showed even higher binding selectivity than did GSL-II, a well known and widely studied lectin for the recognition of terminal GlcNAc residues. Moreover, AAL-2 binds to glycans in a metal-ion-independent manner, whereas Ca^{2+} is required for GSL-II-binding activity (results not shown). The binding activity of AAL-2 was stable under 70 °C and within the pH range 6.0–11.0 (Supplementary Figure S2 at http://www.BiochemJ.org/bj/443/bj4430369add.htm). We compared further the amino acid sequences of AAL-2, GSL-II, WGA and HPA. Surprisingly, amino acid sequences of these GlcNAc-binding lectins showed low similarity to each other, although they shared similar glycan-binding properties (Supplementary Figure S3 at http://www.BiochemJ.org/bj/443/bj4430369add.htm). AAL-2, although newly discovered, has the potential to be utilized as a molecular probe to detect terminal GlcNAc sugars with high binding selectivity in glycan analysis.

Polylactosamine has been reported to be present on the immune co-stimulatory molecules CD28 and CD19. In a previous study [32], B-cells, T-cells and macrophages in the absence of polylactosamines were found to be hypersensitive to stimulation, and SLL was used in the detection of the polylactosamines with at least three lactosamine unit repeats [$(LacNAc)_{n>3}$] [32]. By using glycan arrays to detect the binding profile of lectins, SLL showed high binding selectivity for Neu5Ac (*N*-acetylneuraminic acid)/Fuc (fucose)-$(LacNAc)_3$ and $(LacNAc)_3$ (Consortium for Functional Glycomics database: primscreen_PA_v2_711_09262005). In the present study, the glycan array data showed that AAL-2 bound to GlcNAc-$(LacNAc)_3$ with the highest affinity among the 465 glycan candidates, indicating that AAL-2 recognized polylactosamine $(LacNAc)_3$ with a terminal GlcNAc modification. Overall, the results imply that AAL-2 and SLL would form pairs of complementary probes to monitor changes and modifications of polylactosamine.

GlcNAc has been reported to be aberrantly expressed in several carcinomas, resulting in increased levels and abnormal types of GlcNAc on the cell surface [33,34]. The present study suggests that AAL-2, with high binding selectivity to GlcNAc, could bind to hepatoma cells and induce cell apoptosis. This binding property probably endowed AAL-2 with binding priority to those tumour cells, therefore leading to its potential applications for cancer diagnosis.

AUTHOR CONTRIBUTION

Shuai Jiang, Yi Liang and Hui Sun designed the study. Yijie Chen, Man Wang, Yalin Yin, Yongfu Pan and Bianli Gu carried out the research. Guojun Yu and Yamu Li analysed data. Shuai Jiang, Barry Wong and Hui Sun wrote the paper.

ACKNOWLEDGEMENTS

We thank Ronald L. Schnaar (Johns Hopkins School of Medicine, Baltimore, MD, U.S.A.), Richard D. Cummings (Emory University School of Medicine, Atlanta, GA, U.S.A.), Steven Rosen (University of California, San Francisco, San Francisco, CA, U.S.A.) and Xiangdong Fu (University of California, San Diego, San Diego, CA, U.S.A.) for their suggestions on the glycan array and data analysis. We also thank Yingzhu Zhu (Wuhan University) and Bo Liu (Sichuan University, Chengdu, China) for their critical comments, and Jiajia Xie (Wuhan University) for his technical assistance. The glycan array screening resources were provided by the Consortium for Functional Glycomics (No. GM62116) (Emory University School of Medicine).

FUNDING

This work was supported by the National Key Technologies R&D Program [grant numbers 2009ZX09103-676, 2009ZX09301-014-1 and 2008ZX10001-002], the Natural Science Foundation of China [grant number 81102850], the Major State Basic Research Development Program of China, 973 Program [grant number 2011CB811302], the Chinese 111 project [grant number B06018] and Wuhan municipal project [grant number 201160923296].

REFERENCES

1 Dube, D. H. and Bertozzi, C. R. (2005) Glycans in cancer and inflammation: potential for therapeutics and diagnostics. Nat. Rev. Drug Discovery **4**, 477–488
2 Tanji, T., Ohashi-Kobayashi, A. and Natori, S. (2006) Participation of a galactose-specific C-type lectin in *Drosophila* immunity. Biochem. J. **396**, 127–138
3 Stowell, S. R., Arthur, C. M., Dias-Baruffi, M., Rodrigues, L. C., Gourdine, J. P., Heimburg-Molinaro, J., Ju, T., Molinaro, R. J., Rivera-Marrero, C., Xia, B. et al. (2010) Innate immune lectins kill bacteria expressing blood group antigen. Nat. Med. **16**, 295–301
4 Sharon, N. and Goldstein, I. J. (1998) Lectins: more than insecticides. Science **282**, 1049
5 Kuno, A., Kato, Y., Matsuda, A., Kaneko, M. K., Ito, H., Amano, K., Chiba, Y., Narimatsu, H. and Hirabayashi, J. (2009) Focused differential glycan analysis with the platform antibody-assisted lectin profiling for glycan-related biomarker verification. Mol. Cell. Proteomics **8**, 99–108
6 Tateno, H., Toyoda, M., Saito, S., Onuma, Y., Ito, Y., Hiemori, K., Fukumura, M., Nakasu, A., Nakanishi, M., Ohnuma, K. et al. (2011) Glycome diagnosis of human induced pluripotent stem cells using lectin microarray. J. Biol. Chem. **286**, 20345–20353
7 He, J., Liu, Y., Xie, X., Zhu, T., Soules, M., DiMeco, F., Vescovi, A. L., Fan, X. and Lubman, D. M. (2010) Identification of cell surface glycoprotein markers for glioblastoma-derived stem-like cells using a lectin microarray and LC–MS/MS approach. J. Proteome Res. **9**, 2565–2572
8 Pilobello, K. T., Slawek, D. E. and Mahal, L. K. (2007) A ratiometric lectin microarray approach to analysis of the dynamic mammalian glycome. Proc. Natl. Acad. Sci. U.S.A. **104**, 11534–11539
9 Kuno, A., Uchiyama, N., Koseki-Kuno, S., Ebe, Y., Takashima, S., Yamada, M. and Hirabayashi, J. (2005) Evanescent-field fluorescence-assisted lectin microarray: a new strategy for glycan profiling. Nat. Methods **2**, 851–856
10 Peumans, W. J., Hao, Q. and Van Damme, E. J. (2001) Ribosome-inactivating proteins from plants: more than RNA N-glycosidases? FASEB J. **15**, 1493–1506
11 Ohyama, C., Hosono, M., Nitta, K., Oh-eda, M., Yoshikawa, K., Habuchi, T., Arai, Y. and Fukuda, M. (2004) Carbohydrate structure and differential binding of prostate specific antigen to *Maackia amurensis* lectin between prostate cancer and benign prostate hypertrophy. Glycobiology **14**, 671–679
12 Markiv, A., Peiris, D., Curley, G. P., Odell, M. and Dwek, M. V. (2011) Identification, cloning and characterization of two *N*-acetylgalactosamine-binding lectins from the albumen gland of *Helix pomatia*. J. Biol. Chem. **286**, 20260–20266
13 Sato, Y., Hirayama, M., Morimoto, K., Yamamoto, N., Okuyama, S. and Hori, K. (2011) High mannose-binding lectin with preference for the cluster of α1-2 mannose from the green alga *Boodlea coacta* is a potent entry inhibitor of HIV-1 and influenza viruses. J. Biol. Chem. **286**, 19446–19458
14 Shahzad-Ul-Hussan, S., Gustchina, E., Ghirlando, R., Clore, G. M. and Bewley, C. A. (2011) Solution structure of the monovalent lectin microvirin in complex with Manα(1-2)Man provides a basis for anti-HIV activity with low toxicity. J. Biol. Chem. **286**, 20788–20796
15 Li, J., Wu, H., Hong, J., Xu, X., Yang, H., Wu, B., Wang, Y., Zhu, J., Lai, R., Jiang, X. et al. (2008) Odorranalectin is a small peptide lectin with potential for drug delivery and targeting. PLoS ONE **3**, e2381
16 Xu, X., Yan, H., Chen, J. and Zhang, X. (2011) Bioactive proteins from mushrooms. Biotechnol. Adv. **29**, 667–674
17 Yu, L., Fernig, D. G., Smith, J. A., Milton, J. D. and Rhodes, J. M. (1993) Reversible inhibition of proliferation of epithelial cell lines by *Agaricus bisporus* (edible mushroom) lectin. Cancer Res. **53**, 4627–4632
18 Zhang, G., Sun, J., Wang, H. and Ng, T. B. (2010) First isolation and characterization of a novel lectin with potent antitumor activity from a *Russula* mushroom. Phytomedicine **17**, 775–781
19 Wang, H. X., Liu, W. K., Ng, T. B., Ooi, V. E. and Chang, S. T. (1996) The immunomodulatory and antitumor activities of lectins from the mushroom *Tricholoma mongolicum*. Immunopharmacology **31**, 205–211
20 Li, Y. R., Liu, Q. H., Wang, H. X. and Ng, T. B. (2008) A novel lectin with potent antitumor, mitogenic and HIV-1 reverse transcriptase inhibitory activities from the edible mushroom *Pleurotus citrinopileatus*. Biochim. Biophys. Acta **1780**, 51–57
21 Kawagishi, H., Nomura, A., Mizuno, T., Kimura, A. and Chiba, S. (1990) Isolation and characterization of a lectin from *Grifola frondosa* fruiting bodies. Biochim. Biophys. Acta **1034**, 247–252
22 Woo, B. H., Lee, J. T., Na, D. H. and Lee, K. C. (2001) Sepharose-unbinding ricin E as a source for ricin A chain immunotoxin. J. Immunol. Methods **249**, 91–98
23 Blixt, O., Head, S., Mondala, T., Scanlan, C., Huflejt, M. E., Alvarez, R., Bryan, M. C., Fazio, F., Calarese, D., Stevens, J. et al. (2004) Printed covalent glycan array for ligand profiling of diverse glycan binding proteins. Proc. Natl. Acad. Sci. U.S.A. **101**, 17033–17038
24 Fouquaert, E., Peumans, W. J., Smith, D. F., Proost, P., Savvides, S. N. and Van Damme, E. J. M. (2008) The "old" *Euonymus europaeus* agglutinin represents a novel family of ubiquitous plant proteins. Plant Physiol. **147**, 1316–1324
25 Sun, H., Zhao, C. G., Tong, X. and Qi, Y. P. (2003) A lectin with mycelia differentiation and antiphytovirus activities from the edible mushroom *Agrocybe aegerita*. J. Biochem. Mol. Biol. **36**, 214–222
26 Jacob, L., Lety, M. A., Bach, J. F. and Louvard, D. (1986) Human systemic lupus erythematosus sera contain antibodies against cell-surface protein(s) that share(s) epitope(s) with DNA. Proc. Natl. Acad. Sci. U.S.A. **83**, 6970–6974
27 Kochibe, N. and Matta, K. L. (1989) Purification and properties of an *N*-acetylglucosamine-specific lectin from *Psathyrella velutina* mushroom. J. Biol. Chem. **264**, 173–177
28 Diyabalanage, T., Mulabagal, V., Mills, G., DeWitt, D. L. and Nair, M. G. (2008) Health-beneficial qualities of the edible mushroom, *Agrocybe aegerita*. Food Chem. **108**, 97–102
29 Liang, Y., Feng, L., Tong, X., Wang, K., Li de, F., Lin, J. C., Tang, Z. J., Liu, H. H., Jiang, S., Guo, L., Wang, D. C. and Sun, H. (2009) Importance of nuclear localization for the apoptosis-induced activity of a fungal galectin AAL (*Agrocybe aegerita* lectin). Biochem. Biophys. Res. Commun. **386**, 437–442
30 Zhao, C., Sun, H., Tong, X. and Qi, Y. (2003) An antitumour lectin from the edible mushroom *Agrocybe aegerita*. Biochem. J. **374**, 321–327
31 Nakamura-Tsuruta, S., Kominami, J., Kamei, M., Koyama, Y., Suzuki, T., Isemura, M. and Hirabayashi, J. (2006) Comparative analysis by frontal affinity chromatography of oligosaccharide specificity of GlcNAc-binding lectins, *Griffonia simplicifolia* lectin-II (GSL-II) and *Boletopsis leucomelas* lectin (BLL). J. Biochem. **140**, 285–291
32 Togayachi, A., Kozono, Y., Ishida, H., Abe, S., Suzuki, N., Tsunoda, Y., Hagiwara, K., Kuno, A., Ohkura, T., Sato, N. et al. (2007) Polylactosamine on glycoproteins influences basal levels of lymphocyte and macrophage activation. Proc. Natl. Acad. Sci. U.S.A. **104**, 15829–15834
33 Wang, L., Huang, J., Jiang, M. and Zheng, X. (2010) AFP computational secreted network construction and analysis between human hepatocellular carcinoma (HCC) and no-tumor hepatitis/cirrhotic liver tissues. Tumour Biol. **31**, 417–425
34 Park, J. H., Nishidate, T., Kijima, K., Ohashi, T., Takegawa, K., Fujikane, T., Hirata, K., Nakamura, Y. and Katagiri, T. (2010) Critical roles of mucin 1 glycosylation by transactivated polypeptide N-acetylgalactosaminyltransferase 6 in mammary carcinogenesis. Cancer Res. **70**, 2759–2769
35 Yoon, S. J., Nakayama, K., Hikita, T., Handa, K. and Hakomori, S. I. (2006) Epidermal growth factor receptor tyrosine kinase is modulated by GM3 interaction with N-linked GlcNAc termini of the receptor. Proc. Natl. Acad. Sci. U.S.A. **103**, 18987–18991
36 Toriniwa, H. and Komiya, T. (2011) Comparison of viral glycosylation using lectin blotting with Vero cell-derived and mouse brain-derived Japanese encephalitis vaccines. Vaccine **29**, 1859–1862

37 Lee, J. E., Mirza, S. P., Didier, D. N., Scalf, M., Olivier, M., Greene, A. S. and Smith, L. M. (2008) Identification of cell surface markers to differentiate rat endothelial and fibroblast cells using lectin arrays and LC–ESI–MS/MS. Anal. Chem. **80**, 8269–8275
38 Menheniott, T. R., Peterson, A. J., O'Connor, L., Lee, K. S., Kalantzis, A., Kondova, I., Bontrop, R. E., Bell, K. M. and Giraud, A. S. (2010) A novel gastrokine, Gkn3, marks gastric atrophy and shows evidence of adaptive gene loss in humans. Gastroenterology **138**, 1823–1835
39 Mohr, D., Frey, S., Fischer, T., Guttler, T. and Gorlich, D. (2009) Characterisation of the passive permeability barrier of nuclear pore complexes. EMBO J. **28**, 2541–2553
40 Vosseller, K., Trinidad, J. C., Chalkley, R. J., Specht, C. G., Thalhammer, A., Lynn, A. J., Snedecor, J. O., Guan, S., Medzihradszky, K. F., Maltby, D. A. et al. (2006) O-linked *N*-acetylglucosamine proteomics of postsynaptic density preparations using lectin weak affinity chromatography and mass spectrometry. Mol. Cell. Proteomics **5**, 923–934
41 Jung, J. G., Kim, D. K., Park, T. S., Lee, S. D., Lim, J. M. and Han, J. Y. (2005) Development of novel markers for the characterization of chicken primordial germ cells. Stem Cells **23**, 689–698
42 James, J. R., White, S. S., Clarke, R. W., Johansen, A. M., Dunne, P. D., Sleep, D. L., Fitzgerald, W. J., Davis, S. J. and Klenerman, D. (2007) Single-molecule level analysis of the subunit composition of the T cell receptor on live T cells. Proc. Natl. Acad. Sci. U.S.A. **104**, 17662–17667
43 Shen, Y., Chen, J., Liu, Q., Feng, C., Gao, X., Wang, L., Zhang, Q. and Jiang, X. (2011) Effect of wheat germ agglutinin density on cellular uptake and toxicity of wheat germ agglutinin conjugated PEG-PLA nanoparticles in Calu-3 cells. Int. J. Pharm. **413**, 184–193
44 Wuhrer, M., Grimm, C., Dennis, R. D., Idris, M. A. and Geyer, R. (2004) The parasitic trematode *Fasciola hepatica* exhibits mammalian-type glycolipids as well as Gal(β1-6)Gal-terminating glycolipids that account for cestode serological cross-reactivity. Glycobiology **14**, 115–126
45 Wilson, R., Chen, C. and Ratcliffe, N. A. (1999) Innate immunity in insects: the role of multiple, endogenous serum lectins in the recognition of foreign invaders in the cockroach, *Blaberus discoidalis*. J. Immunol. **162**, 1590–1596
46 Sanchez, J. F., Lescar, J., Chazalet, V., Audfray, A., Gagnon, J., Alvarez, R., Breton, C., Imberty, A. and Mitchell, E. P. (2006) Biochemical and structural analysis of *Helix pomatia* agglutinin: a hexameric lectin with a novel fold. J. Biol. Chem. **281**, 20171–20180
47 Stowell, S. R., Dias-Baruffi, M., Penttila, L., Renkonen, O., Nyame, A. K. and Cummings, R. D. (2004) Human galectin-1 recognition of poly-*N*-acetyllactosamine and chimeric polysaccharides. Glycobiology **14**, 157–167
48 Schmidt, C., Bezuidenhout, D., Beck, M., Van der Merwe, E., Zilla, P. and Davies, N. (2009) Rapid three-dimensional quantification of VEGF-induced scaffold neovascularisation by microcomputed tomography. Biomaterials **30**, 5959–5968
49 Jung, K., Cho, W. and Regnier, F. E. (2009) Glycoproteomics of plasma based on narrow selectivity lectin affinity chromatography. J. Proteome Res. **8**, 643–650

Received 22 November 2011/28 December 2011; accepted 23 January 2012
Published as BJ Immediate Publication 23 January 2012, doi:10.1042/BJ20112061

Biochem. J. (2012) **443**, 369–378 (Printed in Great Britain) doi:10.1042/BJ20112061

online data

SUPPLEMENTARY ONLINE DATA

A novel lectin from *Agrocybe aegerita* shows high binding selectivity for terminal *N*-acetylglucosamine

Shuai JIANG*, Yijie CHEN*, Man WANG*, Yalin YIN*, Yongfu PAN*, Bianli GU*, Guojun YU*, Yamu LI*, Barry Hon Cheung WONG*, Yi LIANG† and Hui SUN*‡§[1]

*College of Life Sciences, Wuhan University, Wuhan 430072, People's Republic of China, †Department of Clinical Immunology, Guangdong Medical College, Dongguan 523808, People's Republic of China, ‡Key Laboratory of Combinatorial Biosynthesis and Drug Discovery (Wuhan University), Ministry of Education, Wuhan 430071, People's Republic of China, and §State Key Laboratory of Virology, Wuhan University, Wuhan 430072, People's Republic of China

Table S1 Carbohydrate-binding profiles of AAL-2 determined by glycan array analysis

The Table lists the glycans present on the glycan array (Consortium for Functional Glycomics). The carbohydrate-binding profiles of AAL-2 at different concentrations (0.1, 1, 50 and 200 μg/ml) are shown. The glycans binding with more than 5000 RFU are listed according to the glycan-binding profile of AAL-2 at 200 μg/ml. Average RFU represents the degree of binding of fluorescently labelled streptavidin to biotin-labelled AAL-2.

Order	Glycan number	Glycan structure	Average RFU for AAL-2 at 200 μg/ml	50 μg/ml	1 μg/ml	0.1 μg/ml
1	336	GlcNAcα1-4Galβ1-4GlcNAcβ1-3Galβ1-4GlcNAcβ1-3Galβ1-4GlcNAcβ-Sp0	30519	13453	1496	226
2	171	GlcNAcα1-3Galβ1-4GlcNAcβ-Sp8	24487	8139	898	130
3	175	GlcNAcβ1-3(GlcNAcβ1-6)Galβ1-4GlcNAcβ-Sp8	21115	3163	515	96
4	339	GlcNAcα1-4Galβ1-4GlcNAcβ1-3Galβ1-4Glcβ-Sp0	20868	9469	1575	132
5	179	GlcNAcβ1-3Galβ1-4GlcNAcβ-Sp0	19530	7071	1151	94
6	172	GlcNAcα1-6Galβ1-4GlcNAcβ-Sp8	19311	4796	447	38
7	337	GlcNAcα1-4Galβ1-4GlcNAcβ-Sp0	19030	4716	883	65
8	181	GlcNAcβ1-3Galβ1-4GlcNAcβ1-3Galβ1-4GlcNAcβ-Sp0	18737	6858	336	105
9	180	GlcNAcβ1-3Galβ1-4GlcNAcβ-Sp8	17289	8012	1247	20
10	338	GlcNAcα1-4Galβ1-3GlcNAcβ-Sp0	16141	6376	853	106
11	341	GlcNAcα1-4Galβ1-4GlcNAcβ1-3Galβ1-4GlcNAcβ-Sp0	11672	4732	518	73
12	308	GlcNAcβ1-4GlcNAcβ-Sp10	11572	93	6	5
13	94	GalNAcβ1-3GalNAcα-Sp8	11198	450	11	5
14	340	GlcNAcα1-4Galβ1-4GlcNAcβ1-3Galβ1-4(Fucα1-3)GlcNAcβ1-3Galβ1-4(Fucα1-3)GlcNAcβ-Sp0	8758	4730	1265	175
15	88	GlcNAcβ1-3Galβ1-3GalNAcα-Sp8	8504	2809	420	24
16	182	GlcNAcβ1-3Galβ1-4Glcβ-Sp0	8464	2539	411	23
17	178	GlcNAcβ1-3Galβ-Sp8	7339	3033	307	19
18	407	GlcNAcβ1-6(GlcNAcβ1-3)GalNAcα-Sp14	6992	108	9	4
19	309	GlcNAcβ1-4GlcNAcβ-Sp12	6078	26	6	3
20	176	GlcNAcβ1-3GalNAcα-Sp8	5896	1395	49	7
21	177	GlcNAcβ1-3GalNAcα-Sp14	5782	7	7	8
22	190	GlcNAcβ1-6GalNAcα-Sp8	5571	31	7	5
23	17	GlcNAcβ-Sp8	5331	11	4	5
24	174	GlcNAcβ1-3(GlcNAcβ1-6)GalNAcα-Sp8	5309	1136	36	10

The nucleotide sequence data for *Agrocybe aegerita* lectin 2 will appear in the GenBank®, EMBL, DDBJ and GSDB Nucleotide Sequence Databases under accession number JN001164.

The glycan array data of AAL-2 were deposited in the Consortium for Functional Glycomics database with the labels primscreen_3312–primscreen_3315.

[1] To whom correspondence should be addressed (email sunhui@whu.edu.cn).

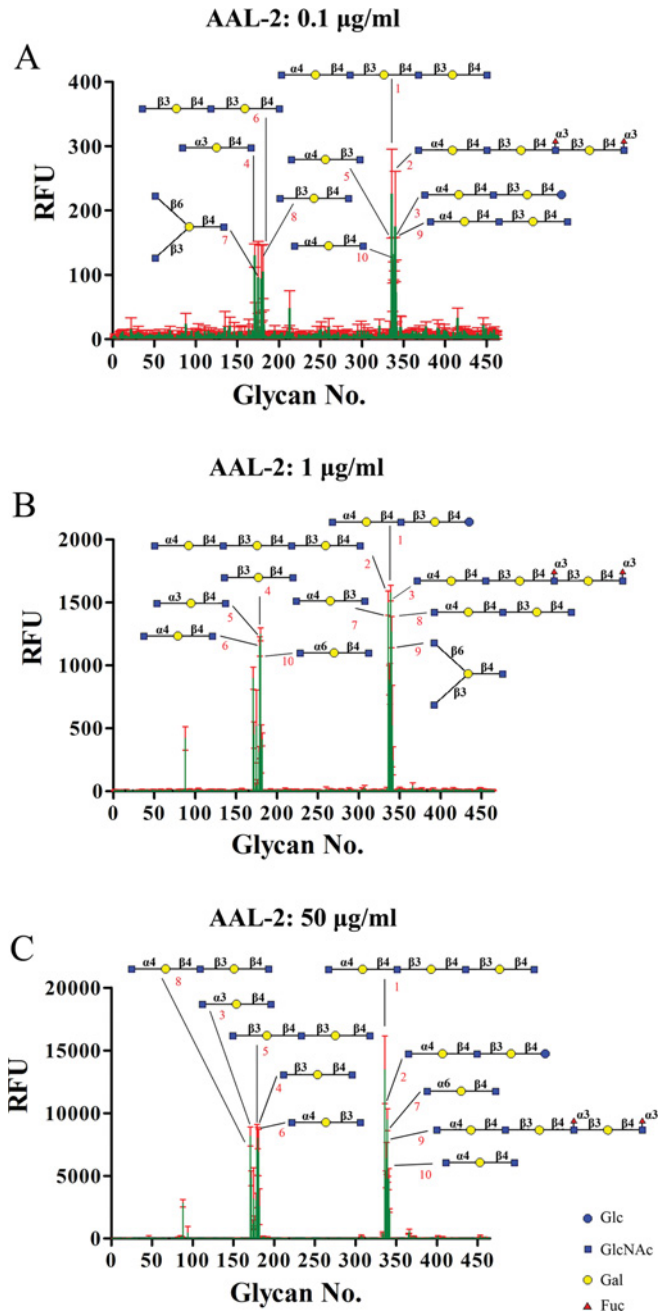

Figure S1 Assessment of AAL-2-binding selectivity by glycan array

A total of 465 glycans were assessed on the array (version 4.1 of the Consortium for Functional Glycomics), and our results showed the top ten binding specific glycans of AAL-2 at 0.1 (**A**), 1 (**B**) and 50 (**C**) μg/ml. Results are means $\pm$ S.E.M. The entire glycan array version is available at http://www.functionalglycomics.org/static/consortium/resources/resourcecoreh14.shtml.

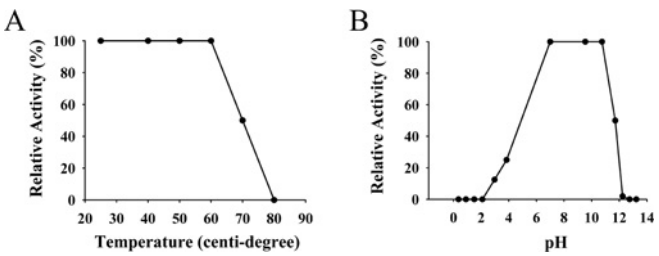

Figure S2 Effects of temperature and pH on the haemagglutination activity of AAL-2

The haemagglutination activity of AAL-2 was tested after treatment at different temperatures (**A**) (centi-degree = °C) and pH (**B**).

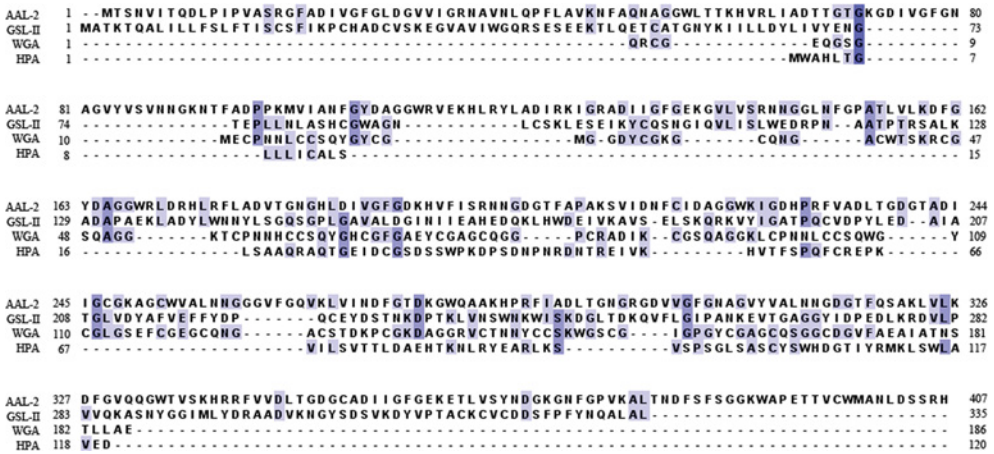

Figure S3 Comparison of the AAL-2 amino acid sequence with other GlcNAc-binding lectins

The AAL-2 amino acid sequence was aligned with GSL-II, WGA and HPA sequences. The background colour denotes similarity between the sequences, with the darker the shade meaning the stronger similarity.

Received 22 November 2011/28 December 2011; accepted 23 January 2012
Published as BJ Immediate Publication 23 January 2012, doi:10.1042/BJ20112061